Cardiovascular, Pulmonary and Renal Pathology

Galectin-3 Expression and Secretion Links Macrophages to the Promotion of Renal Fibrosis

Neil C. Henderson,* Alison C. Mackinnon,*
Sarah L. Farnworth,* Tiina Kipari,*
Christopher Haslett,* John P. Iredale,*
Fu-Tong Liu,[†] Jeremy Hughes,* and Tariq Sethi*

From the Centre for Inflammation Research, The Queen's*
Medical Research Institute, University of Edinburgh, Edinburgh,
United Kingdom; and the Department of Dermatology,[†] School of
Medicine, University of California, Davis, Sacramento, California

Macrophages have been proposed as a key cell type in the pathogenesis of renal fibrosis; however, the mechanism by which macrophages drive fibrosis is still unclear. We show that expression of galectin-3, a β-galactoside-binding lectin, is up-regulated in a mouse model of progressive renal fibrosis (unilateral ureteric obstruction, UUO), and absence of galectin-3 protects against renal myofibroblast accumulation/ activation and fibrosis. Furthermore, specific depletion of macrophages using CD11b-DTR mice reduces fibrosis severity after UUO demonstrating that macrophages are key cells in the pathogenesis of renal fibrosis. Disruption of the galectin-3 gene does not affect macrophage recruitment after UUO, or macrophage proinflammatory cytokine profiles in response to interferon-γ/lipopolysaccharide. In addition, absence of galectin-3 does not affect transforming growth factor-β expression or Smad 2/3 phosphorylation in obstructed kidneys. Adoptive transfer of wild-type but not galectin-3⁻/⁻ macrophages did, however, restore the fibrotic phenotype in galectin-3⁻/⁻ mice. Cross-over experiments using wild-type and galectin-3⁻/⁻ macrophage supernatants and renal fibroblasts confirmed that secretion of galectin-3 by macrophages is critical in the activation of renal fibroblasts to a profibrotic phenotype. Therefore, we demonstrate for the first time that galectin-3 expression and secretion by macrophages is a major mechanism linking macrophages to the promotion of renal fibrosis. *(Am J Pathol 2008, 172:288–298; DOI: 10.2353/ajpath.2008.070726)*

Macrophages are pleiotropic inflammatory cells prominent in both acute and chronic inflammation. In the chronic inflammatory milieu, macrophages interact with other cell types including cells of mesenchymal origin (fibroblasts) that transdifferentiate into matrix-secreting myofibroblasts, with resultant scar formation and disruption of tissue architecture. Advanced renal fibrosis with kidney failure is a major health care burden worldwide,[1] and long-term dialysis or transplantation are the only therapeutic options currently available.[2] Therefore increasing our understanding of the complex interplay between chronic inflammation and progressive fibrosis is a critical step toward the design of rational new treatments.

The importance of macrophages in the wound-healing response has been known for some time. In the 1970s studies on skin wound healing by Leibovich and Ross[3,4] demonstrated that macrophage depletion (with hydrocortisone and anti-macrophage serum) resulted in the delayed appearance of fibroblasts, and their subsequent rate of proliferation was lower than that of controls. More recently, we have shown that selective depletion of macrophages in a model of hepatic inflammation significantly attenuates liver fibrosis.[5] In the kidney there is a striking correlation between tubulointerstitial macrophage infiltration and the severity of fibrosis in human biopsies and the subsequent development and progression of chronic renal failure to end-stage renal failure requiring dialysis.[6,7] Experimental hydronephrosis induced by unilateral ureteric obstruction (UUO) is a clinically relevant animal model because it mimics congenital obstructive nephropathy (the major cause of end-stage renal disease in children[8]), with progression through the different stages of obstructive nephropathy leading to tubulointerstitial fibrosis.[9] Experimental hydronephrosis secondary to UUO is neutrophil- and lymphocyte-independent and is characterized by a marked tubulointerstitial macrophage infiltrate,[10,11] interstitial myofibroblast and tubular epithelial cell proliferation, and progressive scarring with deposi-

tion of extracellular matrix early in the course of the disease.[12,13] Furthermore, the inhibition of tubulointerstitial macrophage recruitment reduces the extent and severity of renal fibrosis[14–18] demonstrating that macrophages play a major role in driving fibrosis after UUO.

Galectin-3 is a β-galactoside-binding animal lectin of ~30 kDa[19] that is highly expressed and secreted by macrophages.[20,21] It is up-regulated when monocytes differentiate into macrophages[21] and down-regulated when macrophages differentiate into dendritic cells.[22] Furthermore, galectin-3 is a potent mitogen for fibroblasts *in vitro*,[23–26] and our previous work has demonstrated that galectin-3 regulates myofibroblast activation and hepatic fibrosis *in vivo*.[27]

We hypothesized that the major tissue source of galectin-3 driving fibrosis is macrophage-derived, and using a model of hydronephrosis we set out to define whether macrophage-derived galectin-3 is a major mechanism linking macrophages to the promotion of renal myofibroblast activation and fibrosis.

Materials and Methods

Tissue culture reagents were purchased from Life Technologies (Paisley, UK). Tissue culture plastics were obtained from Costar (Loughborough, UK) and Falcon (Runcorn, UK). Cytokines and recombinant mouse galectin-3 were purchased from R&D Systems (Abingdon, UK) and Peprotech EC Ltd. (London, UK). The galectin-3 inhibitor bis-[3-deoxy-3-(3-methoxybenzamido)-β-D-galactopyranosyl]-sulfane was provided by U. Nilsson and H. Leffler, University of Lund, Sweden.[28] All other reagents were from Sigma-Aldrich Company Ltd. (Poole, UK) unless otherwise stated.

Animals

Mice were maintained in 12-hour light/12-hour dark cycles with free access to food and water. All procedures were performed in accordance with Home Office guidelines [Animals (Scientific Procedures) Act 1986]. Generation of galectin-3$^{-/-}$ mice by gene-targeting technology has been described previously.[29] As control, age- and sex-matched wild-type littermate mice were used. CD11b-DTR mice were generated and characterized as previously described.[5] Strain-matched controls (FVB/N) were purchased from B and K Ltd. (Hull, UK). All *in vivo* studies had six mice in each experimental group.

Model of Kidney Fibrosis Using UUO

UUO was performed by ligation of the left ureter as described previously.[12] Sham-operated control mice underwent an identical surgical procedure to the UUO mice except ligation of the ureter was not performed. Kidneys were harvested at days 3, 7, and 14 after UUO. For macrophage ablation CD11b-DTR mice and strain-matched control FVB/N mice (six mice per group) received three intravenous injections of either diphtheria toxin (DT) (25 ng/g body weight) or phosphate-buffered

saline after UUO on days 4, 5, and 6. Kidneys were harvested at day 7 and quartered, and samples were then fixed in either methyl Carnoy's reagent (60% methanol, 30% chloroform, 10% glacial acetic acid) for assessment of macrophage infiltration or neutral buffered formalin for immunohistochemistry. Samples were also snap-frozen in liquid nitrogen for real-time reverse transcriptase-polymerase chain reaction (RT-PCR) analysis.

Macrophage Preparation

Bone marrow-derived macrophages (BMDMs) were prepared from wild-type (WT) and galectin-3$^{-/-}$ mice by maturing bone marrow cells in Dulbecco's modified Eagle's medium containing 10% fetal bovine serum and 20% L929 conditioned media for 7 to 9 days as described previously.[30] Mature BMDMs (5×10^5/well) were added to the wells of 24-well plates (or plated onto glass coverslips for immunofluorescence). After 3 hours the wells were washed to remove nonadherent cells. Wells were treated with lipopolysaccharide (LPS) (100 ng/ml) and murine interferon-γ (IFN-γ) (100 U/ml) in serum-free media. After 24 hours of incubation, the supernatants were harvested and clarified by centrifugation at $10,000 \times g$ for 5 minutes and frozen at $-80°C$. *In vivo*-derived peritoneal macrophages were obtained from peritoneal lavage and separated by adhesion onto tissue culture plastic.

Cytokine Analysis

Cytokine release in macrophage supernatants was determined by cytometric bead array, mouse inflammation kit (BD Biosciences, Oxford, UK).

Immunohistochemistry and Immunofluorescence

Paraffin-embedded sections of mouse tissue were processed for immunohistochemistry as described previously,[5] and the following primary antibodies were used: mouse monoclonal anti-α-SMA clone 1A4 (Sigma), rat monoclonal anti-mouse galectin-3 clone 8942F (Cedarlane, Ontario, Canada), and rat anti-mouse F4/80 clone CI:A3-1 (Serotec, Oxford, UK). Methyl Carnoy's-fixed paraffin-embedded sections (4 μm) were used to assess macrophage infiltration (F4/80-positive cells), and sections were visualized and quantified as previously described.[15] The detection of renal fibrocytes was performed by immunofluorescence using specific antibodies against CD34 (Santa Cruz Biotechnology, Santa Cruz, CA), CD45 (Santa Cruz Biotechnology), and type I collagen polyclonal antibody (Chemicon International, Temecula, CA). CD34, CD45, and collagen I immunofluorescence staining of formalin-fixed sections was performed using species-specific Alexa-568- and Alexa-488-conjugated secondary antibodies and fluorescence microscopy (Carl Zeiss Ltd., Welwyn Garden City, UK). BMDMs plated on glass coverslips were washed and fixed in 3% paraformaldehyde and subjected to indirect immunofluorescence with

anti-galectin-3-fluorescein isothiocyanate antibody and then anti-fluorescein isothiocyanate-Alexa-488 antibody. Nuclei were labeled with 4,6-diamidino-2-phenylindole.

Determination of Interstitial Fibrosis of the Renal Cortex

Renal fibrosis was visualized microscopically and quantified with the use of a picrosirius red stain as described previously.[5] Digital image analysis was used to quantitate the amount of red-stained collagen fibers. Morphometric measurements of 10-μm sections stained with picrosirius red were made using OpenLab software (Improvision, Coventry, UK). Twelve nonoverlapping fields at $\times$400 magnification from each section (captured with a Leica DMLB microscope, Leica DC300 camera, and Leica image manager; Leica, Milton Keynes, UK) were analyzed in a blinded manner. Each captured field was analyzed by separation into red, green, and blue (RGB) filters, and the red area was mathematically divided by the red, green, and blue (RGB) area and multiplied by 100%. This represents the percentage area staining positively for collagen fibers, providing a quantitative value on a continuous scale.

Western Blotting

Western blot analysis was undertaken using the following primary antibodies: mouse monoclonal anti-α-smooth muscle actin (SMA) antibody clone 1A4 (Sigma), mouse monoclonal anti-galectin-3 antibody clone A3A12 (Alexis Biochemicals, Nottingham, UK), rabbit polyclonal anti-phospho-Smad2 and anti-phospho-Smad3 (Biosource, Paisley, UK), and goat polyclonal total Smad2/3 antibody (Santa Cruz Biotechnology).

Real-Time RT-PCR

Total RNA from whole kidney was reverse-transcribed into cDNA using random hexamers (Applied Biosystems, Warrington, UK). Mouse primers and probes were as follows: galectin-3: forward 5′-TTGAAGCTGACCACT-TCAAGGTT-3′, reverse 5′-AGGTTCTTCATCCGATGGT-TGT-3′, probe FAM 5′-CGGTCAACGATGCTCACCTACT-GCA-3′ TAMRA; α-SMA: forward 5′-TCAGCGCCTCCA-GTTCCT-3′, reverse 5′-AAAAAAAACCACGAGTAACA-AATCAA-3′; probe FAM 5′-TCCAAA TCATTCCTGC-CCA-3′ TAMRA; procollagen(I): forward 5′-TTCACCTA-CAGCACGCTTGTG-3′, reverse 5′-GATGACTGTCTTGC-CCCAAGTT-3′, probe FAM 5′-ATGGCTGCACGAGTC-ACA-3′ TAMRA; transforming growth factor (TGF)-β: forward 5′-CACCGGAGAGCCCTGGATA-3′, reverse 5′-TG-TACAGCTGCCGCACACA-3′, probe FAM 5′-CAACTAT-TGCTTCAGCTCCACAGAGAAGAACTG-3′ TAMRA. 18S rRNA TaqMan primer probe mix was purchased from Applied Biosystems.

Adoptive Transfer

Mature BMDMs (day 7) were prelabeled with fluorescent Cell-Tracker Orange as per the manufacturers instruc-

tions (Molecular Probes, Eugene, OR). Galectin-3$^{-/-}$ mice underwent UUO surgery at day 0 and received 5 $\times$ 10^6 WT or galectin-3$^{-/-}$ BMDMs at days 1, 3, and 5 intravenously. Tissues were harvested on day 7 including both UUO and contralateral kidney, liver, spleen, and lung.

Isolation of Renal Fibroblasts and Crossover Experiments

Primary cultures of renal fibroblasts were isolated by trypsin digestion (0.25% for 2 hours at 37°C) of minced normal mouse kidneys, and digests were passed through a 20-μm cell strainer (Becton Dickinson, Oxford, UK) to remove glomeruli. Cells were cultured undisturbed in Dulbecco's modified Eagle's medium containing 15% fetal calf serum for 8 days until cells were confluent. Renal fibroblasts were used at passage 2. Mature BMDMs (1 $\times$ 10^6 cells) were plated in six-well tissue culture dishes and incubated in 1 ml of serum-free media for 48 hours. Conditioned media from BMDMs (0.5 ml) or control media were added to 0.5 ml of renal fibroblasts (4 $\times$ 10^4 cells). Cells were incubated for a further 48 hours (final fetal calf serum concentration, 7.5%) before lysis and Western analysis.

Statistical Analysis

Results are presented as means $\pm$ SEM. Significance of the differences between means was assessed using one-way analysis of variance or two-tailed Student's t-test. Values of $P < 0.05$ were considered significant. Unless stated otherwise, studies were performed on three to six independent occasions.

Results

Galectin-3 Expression Is Up-Regulated in a Mouse Model of Progressive Renal Fibrosis (UUO)

Galectin-3 expression was analyzed in a well established experimental model of progressive renal fibrosis (UUO). Galectin-3 expression was markedly increased in the renal interstitium and tubular epithelium after UUO compared with the control sham-operated group (Figure 1, a and b). This increase in galectin-3 expression was confirmed by real-time PCR of whole kidney tissue (Figure 1c, $P < 0.001$).
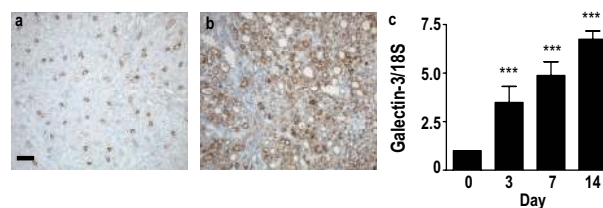

Figure 1. Galectin-3 expression is up-regulated in a mouse model of progressive renal fibrosis (UUO). Galectin-3 expression in tubular epithelium in sham-operated mouse kidney (**a**) and after 14 days of UUO (**b**). **c:** Real-time PCR quantification of galectin-3 expression in whole kidney homogenates from control sham-operated (day 0) and at 3, 7, and 14 days after UUO. ***$P < 0.0001$ compared with control. Scale bar = 100 μm.

Absence of Galectin-3 Protects against Renal Fibrosis

The significance of the induction of galectin-3 expression in the development of renal fibrosis was examined using the UUO model of progressive renal scarring. Renal collagen deposition was stained with picrosirius red (Figure 2, a and b) and quantified using digital image analysis. Significantly reduced collagen deposition was observed in the galectin-3$^{-/-}$ mice compared with WT ($P < 0.05$, Figure 2c). Furthermore transcripts for procollagen (I) were also reduced in the galectin-3$^{-/-}$ group compared with WT animals (Figure 2d, $P < 0.05$). Immunohistochemical examination revealed markedly reduced α-SMA positivity (a marker of activated myofibroblasts, a key cell type involved in extra-

cellular matrix production and scarring in the kidney) in galectin-3$^{-/-}$ compared with WT mice in the UUO model (Figure 2, e and f). α-SMA was quantified using digital image analysis, and significantly less α-SMA staining occurred in the galectin-3$^{-/-}$ mice compared with WT (Figure 2g, $P < 0.05$). α-SMA mRNA transcripts, as assessed by real-time PCR, were significantly decreased in the galectin-3$^{-/-}$ mice compared with WT animals (Figure 2h, $P < 0.01$). Therefore absence of the galectin-3 gene protects against renal fibrosis after UUO.

Specific Depletion of Macrophages Reduces Fibrosis Severity after UUO

Previous studies in which macrophage recruitment to the kidney was inhibited have suggested a role for macrophages in the development of renal fibrosis.[14–18] However, a number of the approaches used do not deplete macrophages specifically, and some deplete neutrophils simultaneously, thereby making interpretation of some of the results more difficult.[31,32] We used the CD11b-DTR mouse[5,33,34] to investigate further the role of macrophages in the evolution of tubulointerstitial scarring. The administration of DT to CD11b-DTR mice specifically ablates monocytes and macrophages.[5,34] Immunostaining for macrophages confirmed marked depletion of macrophages in DT-treated mice (Figure 3, a–c) compared to vehicle-treated control mice. We confirmed previous data showing that the numbers of circulating neutrophils, eosinophils, and lymphocytes are not affected by DT treatment in the DTR mouse by flow cytometry (data not shown)[5,33] Macrophage ablation significantly reduced myofibroblast activation and decreased fibrosis as characterized by reduced α-SMA (Figure 3, d–f) and collagen expression (Figure 3, g–i), confirming an important mechanistic role for macrophages in tubulointerstitial scarring after UUO. Circulating fibrocytes derived from the bone marrow have also been shown to contribute to renal fibrosis.[35] Therefore we assessed whether administration of diphtheria-toxin (DT) in our macrophage depletion model had any effect on fibrocyte recruitment to the kidney after UUO. Figure 4 demonstrates that DT treatment did not significantly deplete kidney fibrocyte recruitment after UUO compared with non-DT controls. These results demonstrate that the development of tubulointerstitial fibrosis after UUO is macrophage-dependent.
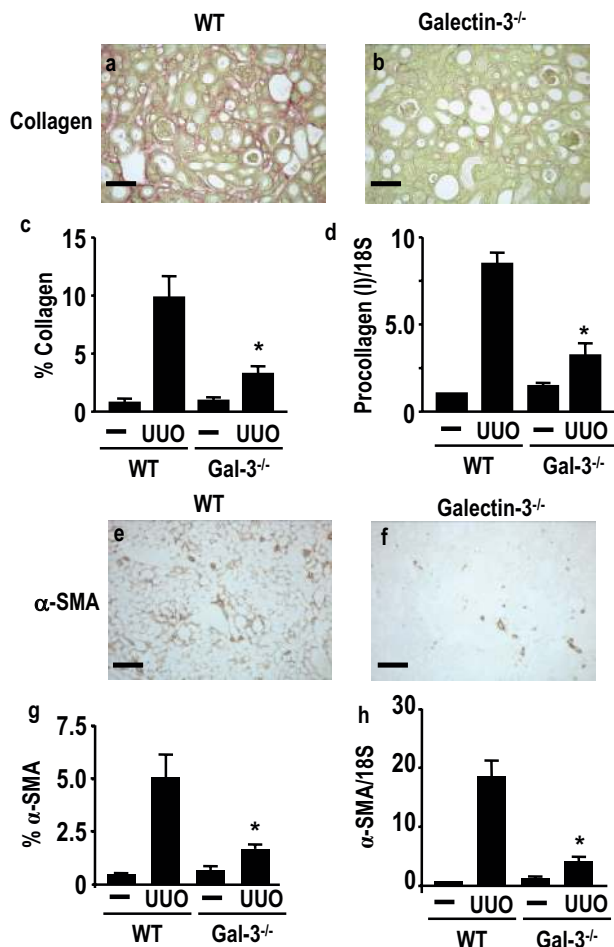

Figure 2. Absence of galectin-3 protects against renal fibrosis. Mice underwent control (sham operation) or UUO and were sacrificed at 7 days ($n = 6$ mice in each group). **a–c:** Renal collagen deposition was examined by picrosirius red staining (**a, b**) and quantified using digital image analysis (**c**). **c:** Significantly reduced collagen deposition was observed in the galectin-3$^{-/-}$ mice compared with WT 7 days after ureteral ligation (*$P < 0.05$). **d:** Furthermore, transcripts for procollagen (I) were also reduced in the galectin-3$^{-/-}$ group compared with WT animals (*$P < 0.05$). **e** and **f:** Immunohistochemistry revealed markedly reduced α-SMA positivity (a marker of myofibroblast activation) in galectin-3$^{-/-}$ compared with WT mice 7 days after ureteral ligation. **g:** α-SMA was quantified using digital image analysis, and significantly less α-SMA staining occurred in the galectin-3$^{-/-}$ mice compared with WT (*$P < 0.05$). **h:** α-SMA mRNA transcripts, as assessed by real-time RT-PCR, were significantly decreased in the galectin-3$^{-/-}$ mice compared with WT animals (*$P < 0.01$). Scale bars = 100 μm.

Disruption of the Galectin-3 Gene Does Not Affect Macrophage Recruitment after UUO or Macrophage Proinflammatory Cytokine Profiles in Response to IFN-γ/LPS

UUO induces severe tubulointerstitial renal injury characterized by a marked interstitial mononuclear cell infiltrate with interstitial myofibroblast and tubular epithelial cell proliferation and deposition of extracellular matrix.[10,11] Because the development of tubulointerstitial fibrosis after UUO is macrophage-dependent, we assessed whether defective mac-
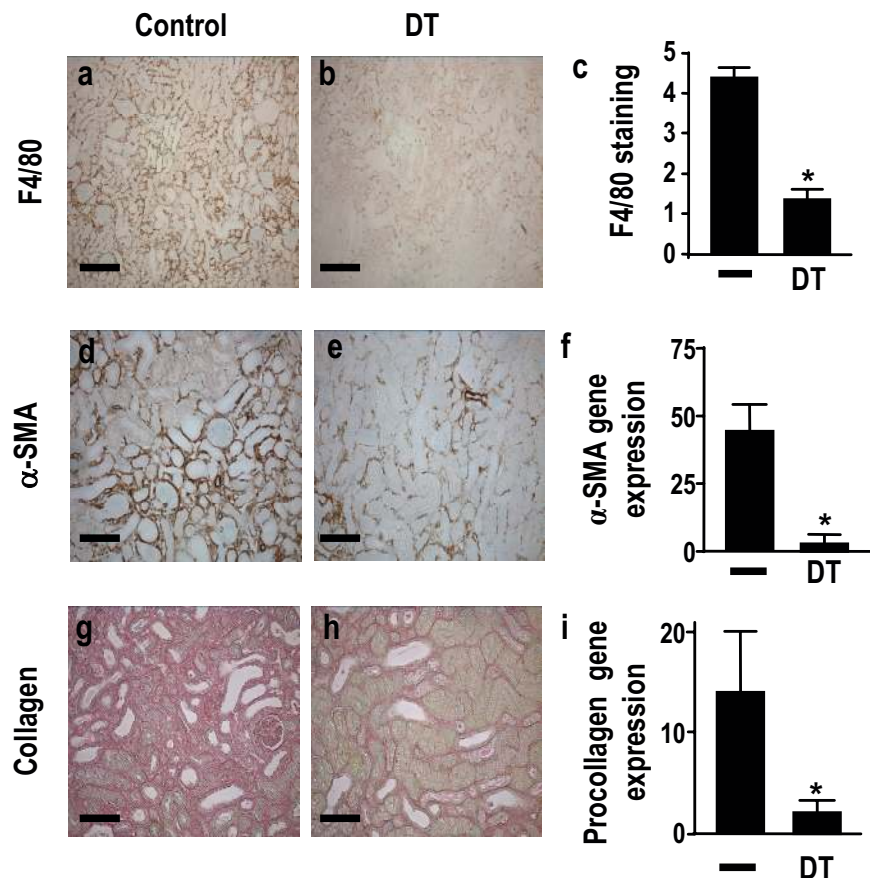
Figure 3. Macrophage ablation by DT reduces renal fibrosis after UUO. Mice underwent UUO and received DT or control vehicle after ureteric ligation ($n = 6$ mice in each group) as described in Materials and Methods. Kidneys were harvested at day 7, and immunostaining was performed for the specific macrophage marker F4/80 (**a**, **b**), α-SMA (**d**, **e**), and collagen (**g**, **h**) in vehicle control-treated (**left**) and DT-treated (**right**) mice. **c:** Quantification of F4/80 staining (macrophage infiltration) by digital image analysis. Real-time RT-PCR quantitation of α-SMA (**f**) and procollagen (I) expression (**i**) in vehicle- and DT-treated mice. *$P < 0.05$ compared to vehicle treated mice. Scale bars = 100 μm.

rophage recruitment in galectin-3$^{-/-}$ mice was responsible for the reduction in renal fibrosis observed after UUO. Figure 5, a–d, shows hematoxylin and eosin (H&E) staining of kidneys from WT and galectin-3$^{-/-}$ mice after sham operation or UUO for 3 days. Renal macrophages were stained with F4/80 (Figure 5, e–h) and quantitated by digital image analysis. Macrophage recruitment was similar in WT and galectin-3$^{-/-}$ mice at all time points studied (days 0, 3, 7, and 14) (Figure 5i). We then examined the cytokine response of BMDMs and *in vivo*-differentiated WT and galectin-3$^{-/-}$ peritoneal macrophages to stimulation with IFN-γ/LPS. There was no significant difference in interleukin (IL)-6 or tumor necrosis factor (TNF)-α release in response to IFN-γ/LPS in BMDMs or *in vivo*-differentiated peritoneal

macrophages isolated from galectin-3$^{-/-}$ or WT mice (Figure 5, j–m). These data demonstrate that the difference in renal fibrosis observed between the two genotypes is not secondary to a difference in the number of macrophages recruited or the macrophage proinflammatory cytokine profile in response to activation with IFN-γ/LPS.

Disruption of the Galectin-3 Gene Does Not Affect TGF-β Expression or Smad 2/3 Phosphorylation in Obstructed Kidneys

Previous studies have implicated TGF-β as an important mediator of fibrosis in the kidney.[36,37] However, mecha-
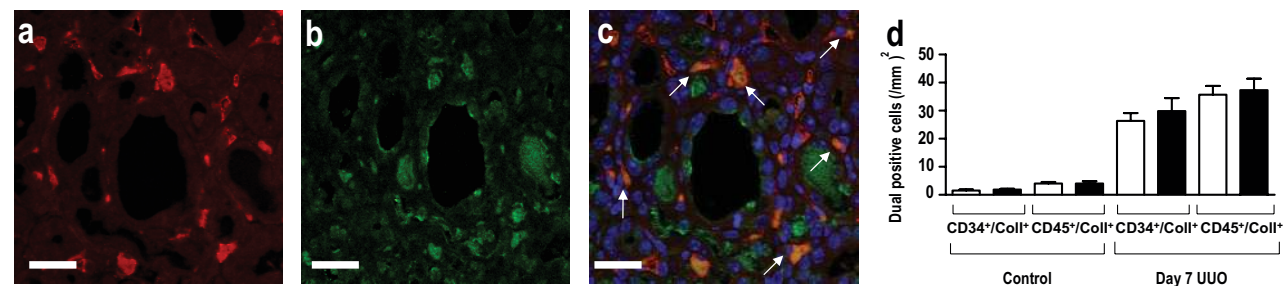

Figure 4. Macrophage ablation by DT does not affect recruitment of CD34$^+$/ColI$^+$ and CD45$^+$/ColI$^+$ fibrocytes after UUO. **a:** CD34; **b:** ColI; **c:** merged. **Arrows** indicate CD34$^+$/ColI$^+$ fibrocytes. **d:** The number of infiltrating fibrocytes (CD34$^+$/ColI$^+$ and CD45$^+$/ColI$^+$) increased at day 7 after UUO, with no significant difference in infiltrating fibrocyte numbers between non-DT-treated (**white bars**) and DT-treated (**black bars**) mice. Day 7 UUO DT$^-$CD34$^+$/ColI$^+$, 26.33 ± 2.8 per mm^2; day 7 UUO DT$^+$CD34$^+$/ColI$^+$, 29.83 ± 4.7 per mm^2 ($n = 6$ mice in each group, $P =$ NS). Day 7 UUO DT$^-$CD45$^+$/ColI$^+$, 35.67 ± 3.2 per mm^2 ($n = 6$), day 7 UUO DT$^+$ CD45$^+$/ColI$^+$, 37.3 ± 4.1 per mm^2 ($n = 6$ mice in each group, $P =$ NS). Values are the mean ± SEM. Scale bars = 100 μm.
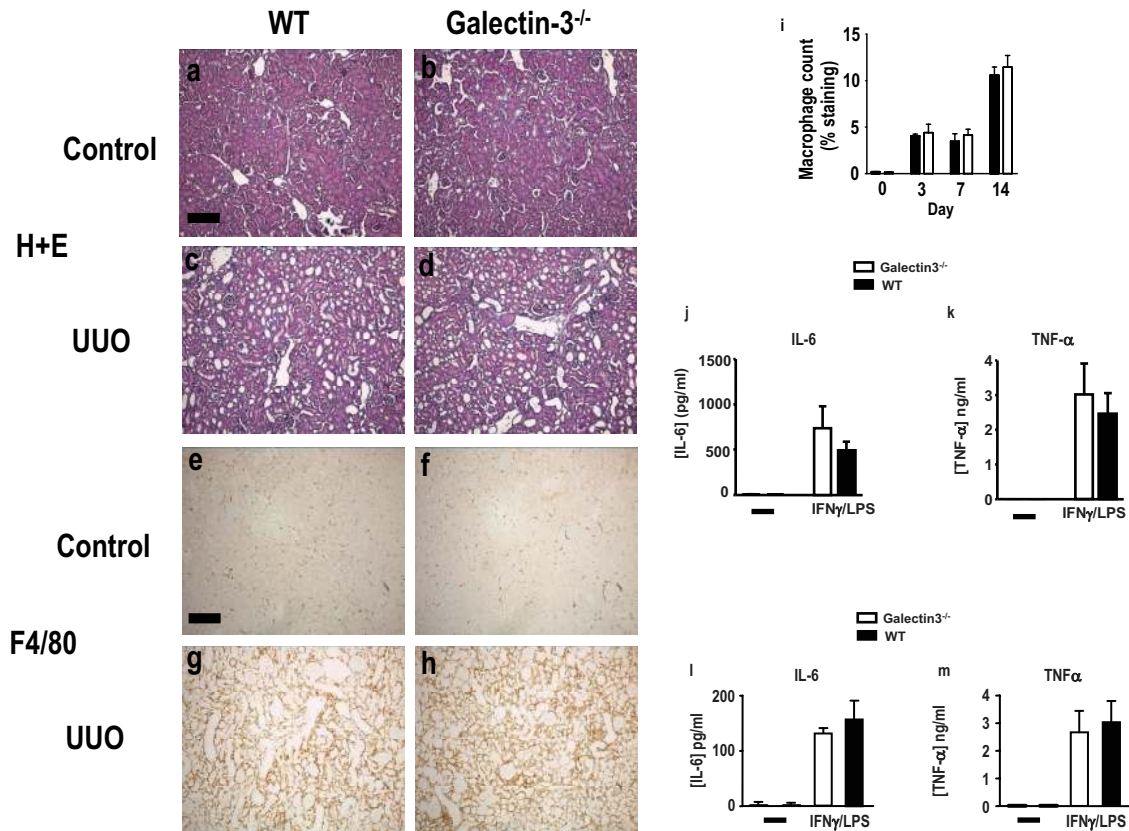
Figure 5. Disruption of the galectin-3 gene does not affect macrophage recruitment after UUO or macrophage proinflammatory cytokine profiles in response to IFN-γ/LPS. **a–d:** H&E staining of kidneys from WT and galectin-3$^{-/-}$ mice 3 days after control sham operation or UUO. Renal macrophages were stained with F4/80 (**e–h**) and quantitated by digital image analysis (**i**). Macrophage recruitment was similar in WT and galectin-3$^{-/-}$ mice at all time points studied after UUO (days 0, 3, 7, and 14) ($n = 6$ mice in each group, $P =$ NS). BMDMs and peritoneal macrophages were stimulated with IFN-γ (100 U/ml) for 48 hours, and LPS (100 ng/ml) was added for the last 24 hours. BMDM supernatants were assayed for IL-6 (**j**) and TNF-α (**k**) (galectin-3$^{-/-}$, **open bar**s; WT, **filled bars**). Peritoneal macrophage supernatants were assayed for IL-6 (**l**) and TNF-α (**m**) (galectin-3$^{-/-}$, **open bars**; WT, **filled bars**). The results represent the mean ± SEM of three experiments ($P =$ NS). Scale bars = 100 μm.

nisms of renal fibrosis also exist that are TGF-β-independent.[38] Therefore we examined whether decreased levels of TGF-β expression in the kidney may be responsible for the observed reduction in renal myofibroblast accumulation/activation and collagen synthesis in galectin-3$^{-/-}$ kidneys compared to WT after UUO. WT and galectin-3$^{-/-}$ mice underwent left UUO and kidneys were harvested at days 3, 7, and 14. TGF-β mRNA expression (analyzed by real-time quantitative PCR of renal tissue) was markedly elevated compared to control after UUO at days 3, 7, and 14 (Figure 6, a–c). However, there was no significant difference in renal TGF-β mRNA expression between WT and galectin-3$^{-/-}$ mice after UUO at any of the time points studied (Figure 6, a–c). In the presence of TGF-β ligand, Smad2 and Smad3, of the receptor-activated Smad family of transcriptional activators, are phosphorylated directly by the TGF-β receptor I kinase.[39] Therefore we measured pSmad2 and pSmad3 expression in lysates from control and UUO kidneys (Figure 6d). There was no significant difference in Smad2 or Smad3 phosphorylation between WT and galectin-3$^{-/-}$ mice (Figure 6, d and e). Therefore disruption of the galectin-3 gene blocks renal fibrosis despite similar expression levels of TGF-β and Smad 2/3 phosphorylation.

Macrophage-Derived Galectin-3 Drives Myofibroblast Accumulation/Activation in the Kidney after UUO

Macrophages have abundant galectin-3 within their nucleus and cytoplasm (Figure 7a) and are able to secrete substantial amounts of galectin-3 into the supernatant in cell culture (Figure 7b). We hypothesized that a major cellular source of galectin-3 during tissue inflammation and fibrosis is the macrophage, and secretion of galectin-3 by macrophages drives myofibroblast activation and renal fibrosis. To test this hypothesis, we adoptively transferred WT and galectin-3$^{-/-}$ macrophages into galectin-3$^{-/-}$ mice after UUO. WT and galectin-3$^{-/-}$ BMDMs were prelabeled with fluorescent Cell Tracker Orange and adoptively transferred into galectin-3$^{-/-}$ mice after UUO (Figure 7, c and d). Kidneys were harvested at day 7 after UUO, when we and others have shown that fibrosis can be observed.[35,40] Infiltration of WT or galectin-3$^{-/-}$ macrophages to the cortex of the obstructed kidneys was quantified by digital image analysis. The recruitment of WT or galectin-3$^{-/-}$ macrophages to the kidneys was comparable (Figure 7, e, f, and k). We also
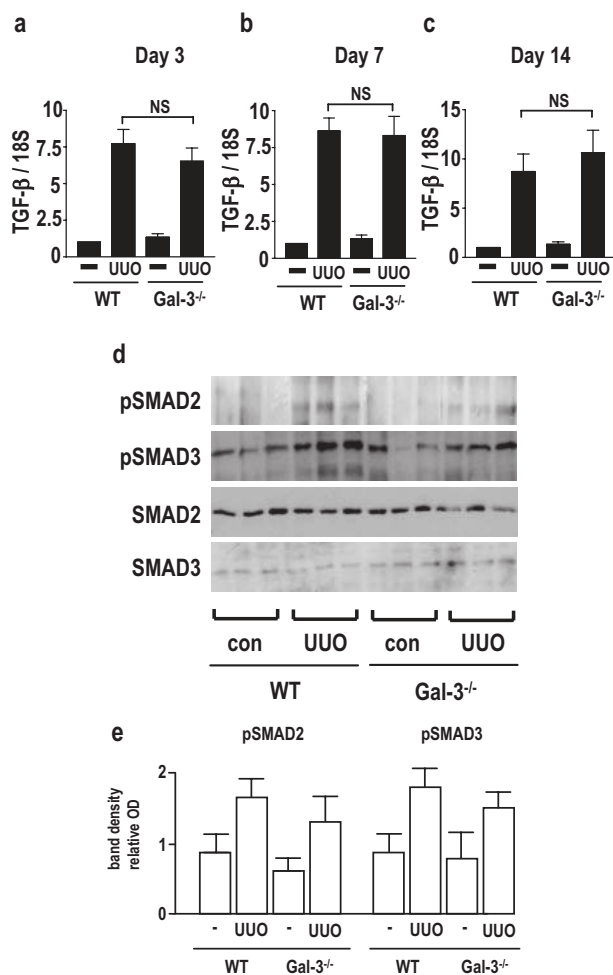
Figure 6. Disruption of the galectin-3 gene does not affect TGF-β expression or Smad 2/3 phosphorylation in obstructed kidneys. WT and galectin-3$^{-/-}$ mice underwent UUO, and kidneys were harvested at days 3, 7, and 14. **a–c:** RNA was extracted, and TGF-β gene expression was measured as described in Materials and Methods by real-time RT-PCR. TGF-β mRNA transcripts were markedly elevated compared to control after UUO at days 3, 7, and 14 ($P < 0.01$ compared to control kidney). However, there was no significant difference in renal TGF-β mRNA expression between WT and galectin-3$^{-/-}$ mice after UUO at any of the time points studied. P = NS. **d:** Western blot of pSMAD2 and pSMAD3 expression in lysates from control and UUO kidneys at day 7 (each lane represents a different mouse). **e:** Quantification by optical densitometry using Image J.

examined other major organs for evidence of macrophage engraftment. As expected, low levels of macrophage engraftment were seen in the liver and spleen (reflecting hepatic and splenic anatomy with sinusoidal fenestrations). However, there was no significant macrophage engraftment in the contralateral kidney or lung. Adoptive transfer of WT macrophages drove the accumulation/activation of interstitial myofibroblasts in the UUO kidney as indicated by the significantly increased interstitial expression of α-SMA (assessed using digital image analysis) in contrast to galectin-3$^{-/-}$ macrophages, which did not (Figure 7, g, h, and l). Although α-SMA is also expressed on vascular smooth muscle cells and some α-SMA-positive interstitial cells do not produce collagen, α-SMA is a widely used surrogate marker for renal myofibroblast activation. Our quantitation of α-SMA excluded staining around blood vessels

and only α-SMA-positive interstitial cells were evaluated. Adoptive transfer of WT macrophages also resulted in increased collagen expression in the UUO kidney [assessed by picrosirius red staining, digital image analysis, and RT-PCR for procollagen (I) mRNA expression] (Figure 7, i, j, m, and n). These data demonstrate that macrophage-derived galectin-3 is a major profibrogenic stimulus within the kidney, driving myofibroblast accumulation/activation and collagen expression after UUO.

Galectin-3-Positive Macrophages Promote Renal Fibroblast Activation in Vitro

To dissect further our *in vivo* model *in vitro* and confirm whether secretion of galectin-3 by macrophages is a key regulator involved in renal myofibroblast activation, we used an *in vitro* cross-over model (Figure 8). Galectin-3$^{-/-}$ renal fibroblasts were isolated and incubated with supernatants collected from either WT or galectin-3$^{-/-}$ BMDMs. Before lysis and Western blotting for α-SMA, cells were counted, and no significant difference in cell counts was seen throughout the different conditions analyzed. As expected, mouse recombinant galectin-3 (30 μg/ml) activated galectin-3$^{-/-}$ renal fibroblasts as evidenced by increased α-SMA expression. Furthermore, incubation of galectin-3$^{-/-}$ renal fibroblasts in conditioned media from WT BMDMs but not galectin-3$^{-/-}$ BMDMs resulted in markedly increased α-SMA expression (Figure 8). Galectin-3$^{-/-}$ renal fibroblast activation by WT BMDM-conditioned media was inhibited by the galectin-3 inhibitor [bis-(3-deoxy-3-{3-methoxybenzamido}-β-D-galactopyranosyl)-sulfane[28]], further confirming that galectin-3 expression and secretion by macrophages is an important mechanism in the promotion of the profibrotic phenotype in renal fibroblasts.

Discussion

Macrophages have been proposed as an important cell type in the pathogenesis of renal fibrosis; however, the mechanism by which macrophages drive fibrosis is still unclear. In this study we examined whether galectin-3 is a key mediator linking macrophages to the promotion of renal fibrosis. We have demonstrated the following: 1) galectin-3 expression is up-regulated in a mouse model of progressive renal fibrosis (UUO), and absence of galectin-3 protects against renal myofibroblast accumulation/activation and fibrosis. 2) Specific depletion of macrophages using CD11b-DTR mice reduces fibrosis severity after UUO demonstrating that macrophages are key cells in the pathogenesis of renal fibrosis. 3) Disruption of the galectin-3 gene does not affect macrophage recruitment after UUO or macrophage proinflammatory cytokine profiles in response to IFN-γ/LPS. 4) Absence of galectin-3 does not affect TGF-β expression or Smad 2/3 phosphorylation in obstructed kidneys. 5) Adoptive transfer of wild-type but not galectin-3$^{-/-}$ macrophages restored the fibrotic phenotype in galectin-3$^{-/-}$ mice. 6)
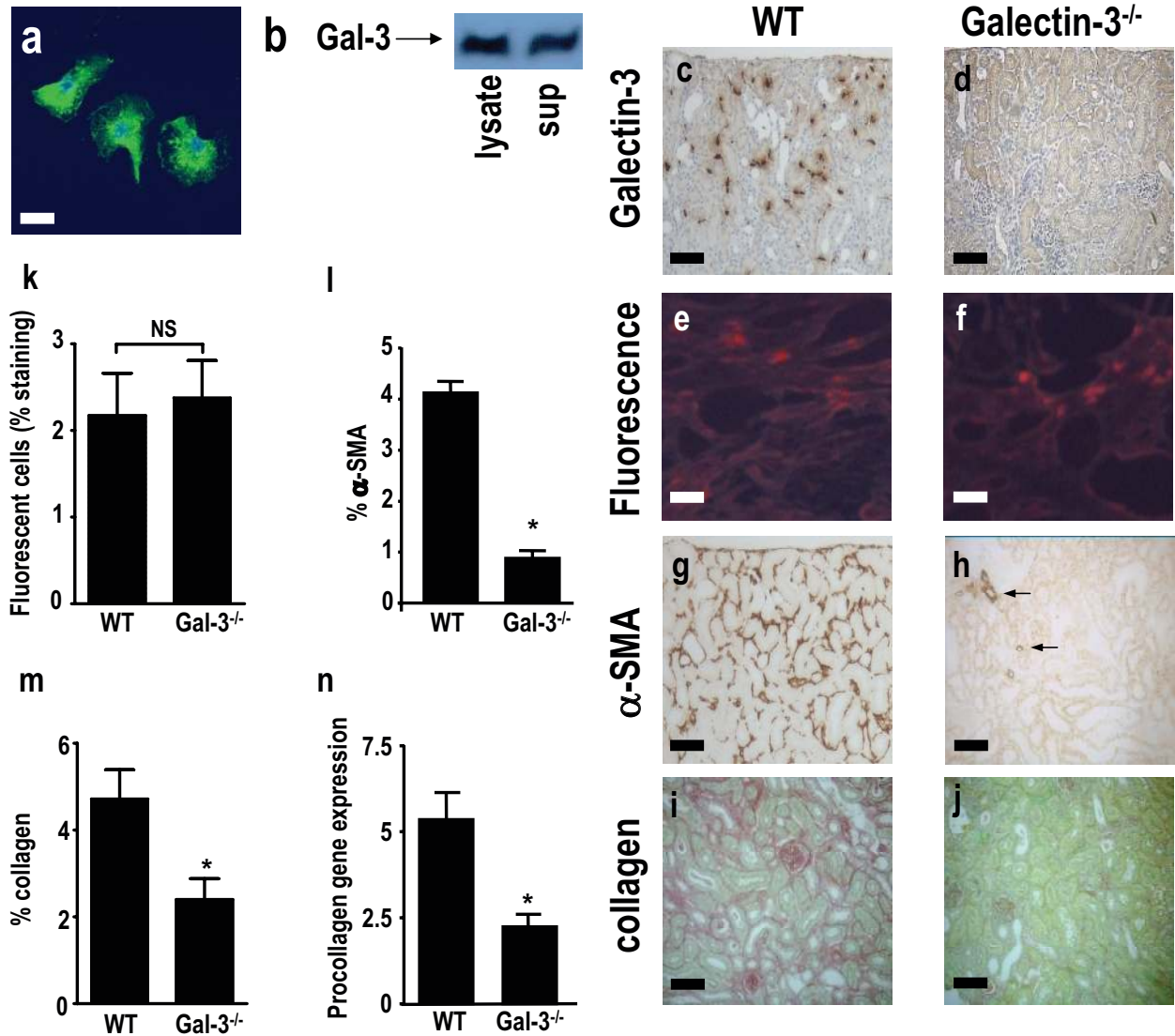
Figure 7. Macrophage-derived galectin-3 drives myofibroblast accumulation/activation in the kidney after UUO. **a:** Galectin-3 immunofluorescence staining of WT BMDMs. Nuclei are labeled with 4,6-diamidino-2-phenylindole. **b:** Representative Western blot of galectin-3 expression in WT BMDM lysate and supernatant. **c–m:** Galectin-3$^{-/-}$ mice underwent UUO, and mature WT or galectin-3$^{-/-}$ BMDMs (5×10^6) were adoptively transferred at days 1, 3, and 5 after ureteric ligation ($n = 6$ in each group) and kidneys were harvested at day 7 after UUO. **c:** Staining of WT macrophages with galectin-3 antibody at day 7 after UUO demonstrating recruitment and engraftment of adoptively transferred WT macrophages. **d:** Control staining of galectin-3$^{-/-}$ macrophages with galectin-3 antibody. **e and f:** Fluorescence microscopy demonstrating Cell Tracker Orange-labeled WT (**e**) and galectin-3$^{-/-}$ (**f**) macrophages recruited and engrafted at day 7 after UUO. **g and h:** α-SMA staining of obstructed kidney after adoptive transfer of WT (**g**) or galectin-3$^{-/-}$ (**h**) macrophages (**arrows** indicate α-SMA staining of blood vessels). **i and j:** Collagen staining (picrosirius red stain) of obstructed kidney after adoptive transfer of WT (**i**) or galectin-3$^{-/-}$ (**j**) macrophages. **k:** Quantitation of recruitment and engraftment of WT and galectin-3$^{-/-}$ macrophages by digital image analysis (P = NS). **l:** Quantitation of α-SMA staining using digital image analysis. **m:** Quantitation of collagen (picrosirius red) staining using digital image analysis. **n:** Quantitation of procollagen (I) gene expression by real-time RT-PCR. *$P < 0.01$ compared to WT adoptively transferred macrophages. Scale bars = 100 μm.

Cross-over experiments using wild-type and galectin-3$^{-/-}$ macrophage supernatants and renal fibroblasts confirmed that secretion of galectin-3 by macrophages is critical in the activation of renal myofibroblasts to a profibrotic phenotype. These novel findings demonstrate that galectin-3 expression and secretion by macrophages is a major mechanism linking macrophages to the promotion of myofibroblast accumulation/activation and renal fibrosis.

Galectin-3 expression and infiltration of macrophages occurred early in our UUO model. Furthermore, as renal fibrosis progresses galectin-3 expression remains up-regulated, and there is a continued increase in macro-phage recruitment. This suggests that the development of renal scarring may be regulated by macrophage galectin-3. Previous studies have shown that inhibition of tubulointerstitial macrophage recruitment reduces the extent and severity of renal fibrosis[14–18] after UUO implying a key role for macrophages in the evolution of renal fibrosis. However, there is also evidence that the role of the macrophage in renal fibrosis may be more complex. Wild-type mice transplanted (after lethal irradiation) with bone marrow from mice lacking Agtr1a (angiotensin II type I receptor) and subjected to 14 days of UUO exhibit more renal fibrosis but less infiltrating macrophages than wild-type mice. These differences were not observed 5
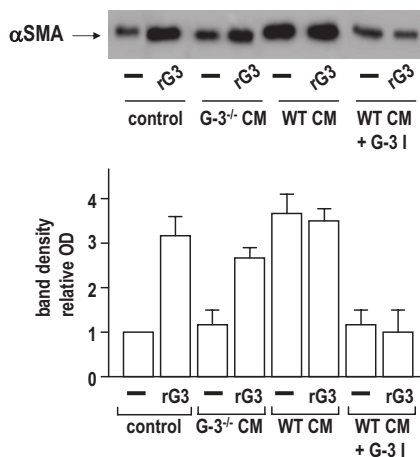
Figure 8. Galectin-3-positive macrophages promote renal fibroblast activation *in vitro*. Mature BMDMs (1×10^6 cells) were plated in six-well tissue culture dishes, incubated in serum-free media, and conditioned media (0.5 ml) was collected after 48 hours. Galectin-3$^{-/-}$ renal fibroblasts were isolated by trypsin digestion as described in Materials and Methods. rG3 refers to recombinant mouse galectin-3 (30 μg/ml). Conditioned media (CM) from BMDMs (0.5 ml) or control media were added to 0.5 ml of renal fibroblasts (4×10^4 cells). WT BMDM-conditioned media were also added in the presence of 5 μmol/L galectin-3 inhibitor (G-3I) [bis-(3-deoxy-3-{3-methoxy-benzamido}-β-D-galactopyranosyl)-sulfane].[28] Cells were incubated for a further 48 hours (final fetal calf serum concentration, 7.5%) before lysis. α-SMA expression in galectin-3$^{-/-}$ renal fibroblast lysates was measured by Western analysis and quantified by optical densitometry using Image J. Results represent the mean ± SEM of three to four independent experiments.

days after UUO.[41] Furthermore adoptive transfer of macrophages at later time-points during the course of UUO-induced renal injury can ameliorate renal fibrosis.[42] Therefore the role of macrophages in renal scarring after UUO may be contextual, with the macrophage able to play both a profibrotic and reparative role at different times, dependent on the stage and degree of renal inflammation and injury.

Therefore to determine further the role of the macrophage in the evolution of renal scarring at day 7 after UUO, we used the CD11b-DTR mouse.[5,33,34] Our data and those of others[5,33] show that DT in the DTR mouse causes specific macrophage depletion and does not affect the numbers of circulating T lymphocytes or granulocytes including neutrophils and eosinophils. Macrophage ablation significantly decreased myofibroblast activation and renal fibrosis, thus confirming a specific role for macrophages in renal scarring after UUO (day 7). However, whereas the central role of the renal myofibroblast in extracellular matrix secretion and kidney fibrosis is widely accepted, interesting data has emerged throughout the last few years that questions the origin and lineage of these cells.[35,43,44] Fibrocytes are a distinct population of circulating cells with fibroblast properties that can specifically enter sites of tissue injury, have a unique cell-surface phenotype expressing hemopoietic and myeloid markers (CD11b$^+$/CD13$^+$/CD34$^+$/CD45RO$^+$/MHC class II$^+$/CD86$^+$), and are capable of secreting collagen.[45,46] Because fibrocytes express CD11b, among other markers, we assessed whether macrophage depletion in our CD11b-DTR mouse had any nonspecific effects on fibrocyte recruitment to the kidney. We found that macrophage depletion using DT had no del-

eterious effects on fibrocyte (CD34/colII^{+ve} and CD45/colII^{+ve}) recruitment, and therefore nonspecific effects on fibrocytes were not responsible for the observed reduction in renal myofibroblast activation and collagen expression. The precise reason why macrophages are specifically depleted in this model and other CD11b-expressing cells are insensitive to DT is unclear but may be attributable to differential gene expression or as a result of lower levels of protein synthesis compared to macrophages.

TGF-β has been implicated as an important mediator of renal fibrosis,[36,37] however TGF-β-independent mechanisms of renal fibrosis have also been reported.[38] We found that galectin-3$^{-/-}$ mice are protected from renal fibrosis after UUO despite developing a macrophage infiltrate comparable to wild-type mice. In-depth analysis of galectin-3$^{-/-}$ and wild-type macrophages demonstrated a similar proinflammatory cytokine response to IFN-γ/LPS, and we have also previously shown that galectin-3$^{-/-}$ BMDMs do not have a deficit in TGF-β production[27] compared to wild type. In our adoptive transfer experiments (Figure 7; adoptively transferred wild-type and galectin-3$^{-/-}$ macrophages into a galectin-3-null background), adoptive transfer of wild-type or galectin-3$^{-/-}$ macrophages after UUO resulted in similar levels of renal Smad2/3 phosphorylation (data not shown). Furthermore, whole tissue renal TGF-β levels and Smad2 and Smad3 phosphorylation increased to a similar extent in wild-type and galectin-3$^{-/-}$ mice after UUO (Figure 6). Therefore despite comparable renal expression of TGF-β and intact TGF-β signaling to Smad 2 and Smad3 in wild-type and galectin-3$^{-/-}$ mice, absence of galectin-3 markedly inhibited fibrosis after UUO, suggesting that TGF-β-mediated renal fibrosis requires galectin-3.

Galectin-3 is a potent activator of fibroblasts isolated from a broad range of tissues including the kidneys, liver, gut, and heart.[25–27,47,48] Infiltration of macrophages is common to almost all forms of adult wound healing and repair, regardless of organ type, and as demonstrated above macrophages appear critical in the promotion of renal fibrosis after UUO. However, the mechanisms that allow macrophages to communicate with extracellular matrix-secreting myofibroblasts and thus drive fibrosis within the chronic inflammatory milieu are still unclear. In a rat model of heart failure, myocardial macrophage galectin-3 is highly up-regulated during the onset of disease, serving to identify animals that later developed rapid heart failure. Furthermore, galectin-3 was associated with cardiac fibroblast proliferation and collagen deposition.[48] Therefore, we hypothesized that the major tissue source of galectin-3 driving renal fibrosis is macrophage derived. The adoptive transfer of wild-type but not galectin-3$^{-/-}$ macrophages resulted in myofibroblast accumulation/activation and collagen deposition. Thus, despite normal recruitment of galectin-3$^{-/-}$ macrophages to obstructed kidneys, they were unable to drive myofibroblast accumulation/activation and fibrosis. Further testing of our hypothesis *in vitro* using cross-over experiments with wild-type and galectin-3$^{-/-}$ macrophage supernatants and galectin-3$^{-/-}$ renal fibroblasts confirmed that galectin-3 secretion by macrophages is a

key event in the activation of renal fibroblasts to a profibrotic phenotype.

These data, together with our previous findings demonstrating an important role for galectin-3 in the development of liver fibrosis,[27] suggest that galectin-3 may play a more general pan-organ role in fibrosis. We have demonstrated a profibrotic signaling axis between macrophages and tissue fibroblasts mediated by galectin-3, which may be broadly applicable to scarring conditions in other organs where chronic inflammation results in the close apposition of these two cell types. Therefore, targeted inhibition of macrophage galectin-3 expression and secretion may result in the development of novel antifibrotic therapies.

Acknowledgments

References

1. El Nahas AM, Bello AK: Chronic kidney disease: the global challenge. Lancet 2005, 365:331–340
2. Sayegh MH, Carpenter CB: Transplantation 50 years later—progress, challenges, and promises. N Engl J Med 2004, 351:2761–2766
3. Leibovich SJ, Ross R: The role of the macrophage in wound repair. A study with hydrocortisone and antimacrophage serum. Am J Pathol 1975, 78:71–100
4. Leibovich SJ, Ross R: A macrophage-dependent factor that stimulates the proliferation of fibroblasts in vitro. Am J Pathol 1976, 84:501–514
5. Duffield JS, Forbes SJ, Constandinou CM, Clay S, Partolina M, Vuthoori S, Wu S, Lang R, Iredale JP: Selective depletion of macrophages reveals distinct, opposing roles during liver injury and repair. J Clin Invest 2005, 115:56–65
6. Bohle A, Muller GA, Wehrmann M, Mackensen-Haen S, Xiao JC: Pathogenesis of chronic renal failure in the primary glomerulopathies, renal vasculopathies, and chronic interstitial nephritides. Kidney Int 1996, 54:S2–S9
7. Becker GJ, Hewitson TD: The role of tubulointerstitial injury in chronic renal failure. Curr Opin Nephrol Hypertens 2000, 9:133–138
8. Roth KS, Koo HP, Spottswood SE, Chan JC: Obstructive uropathy: an important cause of chronic renal failure in children. Clin Pediatr 2002, 45:309–314
9. Bascands JL, Schanstra JP: Obstructive nephropathy: insights from genetically engineered animals. Kidney Int 2005, 68:925–937
10. Schreiner GF, Harris KP, Purkerson ML, Klahr S: Immunological aspects of acute ureteral obstruction: immune cell infiltrate in the kidney. Kidney Int 1988, 34:487–493
11. Diamond JR: Macrophages and progressive renal disease in experimental hydronephrosis. Am J Kidney Dis 1995, 26:133–140
12. Hughes J, Johnson RJ: Role of Fas (CD95) in tubulointerstitial disease induced by unilateral ureteric obstruction. Am J Physiol 1999, 277:F26–F32
13. Diamond JR, van Goor H, Ding G, Engelmyer E: Myofibroblasts in experimental hydronephrosis. Am J Pathol 1995, 146:121–129
14. Ophascharoensuk V, Giachelli CM, Gordon K, Hughes J, Pichler R, Brown P, Liaw L, Schmidt R, Shankland SJ, Alpers CE, Couser WG, Johnson RJ: Obstructive uropathy in the mouse: role of osteopontin in interstitial fibrosis and apoptosis. Kidney Int 1999, 56:571–580
15. Lange-Sperandio B, Cachat F, Thornhill BA, Chevalier RL: Selectins mediate macrophage infiltration in obstructive nephropathy in newborn mice. Kidney Int 2002, 61:516–524
16. Anders HJ, Vielhauer V, Frink M, Linde Y, Cohen CD, Blattner SM, Kretzler M, Strutz F, Mack M, Grone HJ, Onuffer J, Horuk R, Nelson PJ, Schlondorff D: A chemokine receptor CCR-1 antagonist reduces renal fibrosis after unilateral ureter ligation. J Clin Invest 2002, 109:251–259
17. Eis V, Luckow B, Vielhauer V, Siveke JT, Linde Y, Segerer S, Perez De Lema G, Cohen CD, Kretzler M, Mack M, Horuk R, Murphy PM, Gao JL, Hudkins KL, Alpers CE, Grone HJ, Schlondorff D, Anders HJ: Chemokine receptor CCR1 but not CCR5 mediates leukocyte recruitment and subsequent renal fibrosis after unilateral ureteral obstruction. J Am Soc Nephrol 2004, 15:337–347
18. Kitagawa K, Wada T, Furuichi K, Hashimoto H, Ishiwata Y, Asano M, Takeya M, Kuziel WA, Matsushima K, Mukaida N, Yokoyama H: Blockade of CCR2 ameliorates progressive fibrosis in kidney. Am J Pathol 2004, 165:237–246
19. Ho MK, Springer TA: Mac-2, a novel 32,000 Mr mouse macrophage subpopulation-specific antigen defined by monoclonal antibodies. J Immunol 1982, 128:1221–1228
20. Sato S, Hughes RC: Regulation of secretion and surface expression of Mac-2, a galactoside-binding protein of macrophages. J Biol Chem 1994, 269:4424–4430
21. Liu FT, Hsu DK, Zuberi RI, Kuwabara I, Chi EY, Henderson WR Jr: Expression and function of galectin-3, a beta-galactoside-binding lectin, in human monocytes and macrophages. Am J Pathol 1995, 147:1016–1028
22. Dietz AB, Bulur PA, Knutson GJ, Matasic R, Vuk-Pavlovic S: Maturation of human monocyte-derived dendritic cells studied by microarray hybridization. Biochem Biophys Res Commun 2000, 275:731–738
23. Moutsatsos IK, Wade M, Schindler M, Wang JL: Endogenous lectins from cultured cells: nuclear localization of carbohydrate-binding protein 35 in proliferating 3T3 fibroblasts. Proc Natl Acad Sci USA 1987, 84:6452–6456
24. Inohara H, Akahani S, Raz A: Galectin-3 stimulates cell proliferation. Exp Cell Res 1998, 245:294–302
25. Sasaki S, Bao Q, Hughes RC: Galectin-3 modulates rat mesangial cell proliferation and matrix synthesis during experimental glomerulonephritis induced by anti-Thy1.1 antibodies. J Pathol 1999, 187:481–489
26. Maeda N, Kawada N, Seki S, Arakawa T, Ikeda K, Iwao H, Okuyama H, Hirabayashi J, Kasai K, Yoshizato K: Stimulation of proliferation of rat hepatic stellate cells by galectin-1 and galectin-3 through different intracellular signaling pathways. J Biol Chem 2003, 278:18938–18944
27. Henderson NC, Mackinnon AC, Farnworth SL, Poirier F, Russo FP, Iredale JP, Haslett C, Simpson KJ, Sethi T: Galectin-3 regulates myofibroblast activation and hepatic fibrosis. Proc Natl Acad Sci USA 2006, 103:5060–5065
28. Cumpstey I, Sundin A, Leffler H, Nilsson UJ: C2-symmetrical thiodigalactoside bis-benzamido derivatives as high-affinity inhibitors of galectin-3: efficient lectin inhibition through double arginine-arene interactions. Angew Chem Int Ed Engl 2005, 44:5110–5112
29. Colnot C, Ripoche MA, Milon G, Montagutelli X, Crocker PR, Poirier F: Maintenance of granulocyte numbers during acute peritonitis is defective in galectin-3-null mutant mice. Immunology 1998, 94:290–296
30. Duffield JS, Erwig LP, Wei X, Liew FY, Rees AJ, Savill JS: Activated macrophages direct apoptosis and suppress mitosis of mesangial cells. J Immunol 2000, 164:2110–2119
31. Ikezumi Y, Hurst LA, Masaki T, Atkins RC, Nikolic-Paterson DJ: Adoptive transfer studies demonstrate that macrophages can induce proteinuria and mesangial cell proliferation. Kidney Int 2003, 63:83–95
32. Diamond JR, Pesek-Diamond I: Sublethal X-irradiation during acute puromycin nephrosis prevents late renal injury: role of macrophages. Am J Physiol 1991, 260:F779–F786
33. Duffield JS, Tipping PG, Kipari T, Cailhier JF, Clay S, Lang R, Bonventre JV, Hughes J: Conditional ablation of macrophages halts progression of crescentic glomerulonephritis. Am J Pathol 2005, 167:1207–1219
34. Cailhier JF, Partolina M, Vuthoori S, Wu S, Ko K, Watson S, Savill J, Hughes J, Lang RA: Conditional macrophage ablation demonstrates that resident macrophages initiate acute peritoneal inflammation. J Immunol 2005, 174:2336–2342
35. Sakai N, Wada T, Yokoyama H, Lipp M, Ueha S, Matsushima K, Kaneko S: Secondary lymphoid tissue chemokine (SLC/CCL21)/CCR7 signaling regulates fibrocytes in renal fibrosis. Proc Natl Acad Sci USA 2006, 103:14098–14103
36. Sharma K, Ziyadeh FN: The emerging role of transforming growth factor-beta in kidney diseases. Am J Physiol 1994, 266:F829–F842
37. Sato M, Muragaki Y, Saika S, Roberts AB, Ooshima A: Targeted

disruption of TGF-beta1/Smad3 signaling protects against renal tubulointerstitial fibrosis induced by unilateral ureteral obstruction. J Clin Invest 2003, 112:1486–1494

38. Ma LJ, Yang H, Gaspert A, Carlesso G, Barty MM, Davidson JM, Sheppard D, Fogo AB: Transforming growth factor-beta-dependent and -independent pathways of induction of tubulointerstitial fibrosis in beta6(−/−) mice. Am J Pathol 2003, 163:1261–1273

39. Heldin CH, Miyazono K, ten Dijke P: TGF-beta signalling from cell membrane to nucleus through SMAD proteins. Nature 1997, 390:465–471

40. Kipari T, Cailhier JF, Ferenbach D, Watson S, Houlberg K, Walbaum D, Clay S, Savill J, Hughes J: Nitric oxide is an important mediator of renal tubular epithelial cell death in vitro and in murine experimental hydronephrosis. Am J Pathol 2006, 169:388–399

41. Nishida M, Fujinaka H, Matsusaka T, Price J, Kon V, Fogo AB, Davidson JM, Linton MF, Fazio S, Homma T, Yoshida H, Ichikawa I: Absence of angiotensin II type 1 receptor in bone marrow-derived cells is detrimental in the evolution of renal fibrosis. J Clin Invest 2002, 110:1859–1868

42. Nishida M, Okumura Y, Fujimoto S, Shiraishi I, Itoi T, Hamaoka K: Adoptive transfer of macrophages ameliorates renal fibrosis in mice. Biochem Biophys Res Commun 2005, 332:11–16

43. Iwano M, Plieth D, Danoff TM, Xue C, Okada H, Neilson EG: Evidence that fibroblasts derive from epithelium during tissue fibrosis. J Clin Invest 2002, 110:341–350

44. Zeisberg M, Hanai J, Sugimoto H, Mammoto T, Charytan D, Strutz F, Kalluri R: BMP-7 counteracts TGF-beta1-induced epithelial-to-mesenchymal transition and reverses chronic renal injury. Nat Med 2003, 9:964–968

45. Metz CN: Fibrocytes: a unique cell population implicated in wound healing. Cell Mol Life Sci 2003, 60:1342–1350

46. Chesney J, Metz C, Stavitsky AB, Bacher M, Bucala R: Regulated production of type I collagen and inflammatory cytokines by peripheral blood fibrocytes. J Immunol 1998, 160:419–425

47. Lippert E, Falk W, Bataille F, Kaehne T, Naumann M, Goeke M, Herfarth H, Schoelmerich J, Rogler G: Soluble galectin-3 is a strong, colonic epithelial-cell-derived, lamina propria fibroblast-stimulating factor. Gut 2007, 56:43–51

48. Sharma UC, Pokharel S, van Brakel TJ, van Berlo JH, Cleutjens JP, Schroen B, Andre S, Crijns HJ, Gabius HJ, Maessen J, Pinto YM: Galectin-3 marks activated macrophages in failure-prone hypertrophied hearts and contributes to cardiac dysfunction. Circulation 2004, 110:3121–3128